Continuous rate modeling of bacterial stochastic size dynamics

César Nieto,[1,2] César Vargas-García,[3] and Juan M. Pedraza[1,*]
[1]*Department of Physics, Universidad de los Andes, Bogotá 111711, Colombia*
[2]*Department of Electrical and Computer Engineering, University of Delaware, Newark, Delaware 19716, USA*
[3]*Corporacion Colombiana de Investigación Agropecuaria AGROSAVIA, Mosquera 250047, Colombia*

(Received 24 June 2021; accepted 6 October 2021; published 29 October 2021)

Bacterial division is an inherently stochastic process with effects on fluctuations of protein concentration and phenotype variability. Current modeling tools for the stochastic short-term cell-size dynamics are scarce and mainly phenomenological. Here we present a general theoretical approach based on the Chapman-Kolmogorov equation incorporating continuous growth and division events as jump processes. This approach allows us to include different division strategies, noisy growth, and noisy cell splitting. Considering bacteria synchronized from their last division, we predict oscillations in both the central moments of the size distribution and its autocorrelation function. These oscillations, barely discussed in past studies, can arise as a consequence of the discrete time displacement invariance of the system with a period of one doubling time, and they do not disappear when including stochasticity on either division times or size heterogeneity on the starting population but only after inclusion of noise in either growth rate or septum position. This result illustrates the usefulness of having a solid mathematical description that explicitly incorporates the inherent stochasticity in various biological processes, both to understand the process in detail and to evaluate the effect of various sources of variability when creating simplified descriptions.

DOI: 10.1103/PhysRevE.104.044415

I. INTRODUCTION

Recent experiments involving time-lapse microscopy [1], single-cell tracking [2,3], and gene tagging [4] have revealed that stochasticity in cell-size and division events can play an important role in the random fluctuations of biomolecular concentrations [5–9]. This, in turn, has important consequences for phenotype variability and cell heterogeneity in clonal populations [10].

An existing method for describing bacterial size control is based on discrete stochastic maps (DSMs) [11,12]. This is a phenomenological approach that defines the *division strategy* as a map that takes cell size at birth s_b to a targeted cell size at division s_d through a deterministic function $s_d = f(s_b)$ plus stochastic fluctuations that have to be fitted from experiments. DSMs, however, are unable to reproduce cell-size transient dynamics at arbitrary infinitesimal time intervals without further extensions.

A well-known way to solve the continuous dynamics of the distributions describing stochastic processes is based on the Chapman-Kolgomorov equation (CK) [13]. CK solutions correspond to the distributions of all possible stochastic hybrid trajectories at a given time. Among the processes that can be modeled by CK, continuous size growth and division can be included as a jump process with a continuous rate of division. These models are also known as continuous rate models (CRM) [11]. With this type of models, Wang and colleagues [14] proposed a power-law function to explain observations in *Escherichia coli* bacteria, and Osella *et al.* [15] suggested that a convoluted function of size and cycle progression is required. We [16] then proposed a deconvoluted version by introducing division as a multistep process where the occurrence rate of the steps is a function of the size. Recently, some efforts have estimated analytical expression for stationary distributions [17]. Despite these attempts, a complete formalism capturing the stochastic phenomena related to the dynamics of bacterial division was still lacking.

In our previous work [16], we used the theory of CRMs to unify the known division strategies based on DSMs and describe the dynamics of simple gene architectures [5]. We have also presented some preliminary results on simulation techniques based on this framework [18] and basic solutions for some simple ideal examples [19,20]. Here we present the formal, detailed solution for the stochastic size dynamics modeled by the CK equation trying to be as realistic as possible, using both simulations and numerical methods but presenting analytical expressions whenever possible.

To simplify the problem, we consider the dynamics of cells synchronized from their last division. This can easily be done *a posteriori* on experimental data. However, to approach a realistic description we included some effects and sources of noise that had not been incorporated before, such as variability on the starting size or division timing. For this last effect, we use the basic idea of Refs. [19,20], but considering that the jumps are triggered after the occurrence of a certain number of division steps. Although these steps can be associated to the accumulation of FtsZ or other precursor proteins [21,22], the model does not depend on the biochemical details of the

*Correspondence: jmpedraza@uniandes.edu.co

molecules. We also explain how to integrate into the CK equation some other more complex sources of noise such as the noise in splitting position (similarly to the reported in Refs. [17,23]) or cell-to-cell variability in the growth rate (already mentioned in Refs. [24,25]). We end with a discussion of how this approach could be coupled with current simulations of gene expression to obtain more accurate protein dynamics.

II. MODEL DESCRIPTION

In this section, we present the Chapmann-Kolmogorov equation describing the dynamics of the size distribution for growing and dividing bacteria. In our framework, we consider an ever-growing cell population. After each division only one of the descendants of each cell is tracked so that the number of bacteria in the observed population remains constant. This corresponds to experimental setups such as those using *Mother Machine* microfluidics [3,14]. Other works have described the dynamics of this distribution including effects such as the increasing cell number in a microcolony or mother-daughter correlations [20,26–28].

A. The population balance equation

Consider the distribution $p(s;t)$ of sizes s at a given time t. For a population with constant number, $p(s;t)$ can be normalized:

$$\int p(s;t)ds = 1. \tag{1}$$

To describe how this distribution evolves, let us start by considering an individual cell's growth in size s described by

$$ds = g(s;t)dt, \quad s(0) = s_0, \tag{2}$$

where $g(s;t)$ is the size change per unit time and s_0 is the initial cell size. For now, let us consider the deterministic process assuming that all cells have the same s_0. Some studies [20,29,30] have considered $g(s;t)$ as a constant (linear growth), whereas we will focus on an exponential growth ($g(s;t) = \mu s$) with μ being a constant usually called the growth rate.

Since (2) defines a deterministic process, the change in the size distribution $p(s|s_0;t)$ conditioned by the initial size s_0 can be obtained by solving

$$\frac{\partial}{\partial t}p(s|s_0;t) = -\frac{\partial}{\partial s}[g(s;t)p(s|s_0;t)]. \tag{3}$$

Expression (3) is known as the forward Chapman-Kolmogorov equation (CKE) in its differential version [13], and its solution for this deterministic process is given by

$$p(s|s_0;t) = \delta[s - s_{\text{det}}(t)], \tag{4}$$

where $s_{\text{det}}(t) = s_0 e^{\mu t}$ is the solution of Eq. (2) and $\delta(s)$ is the Dirac delta distribution.

Considering division as a jump process, during splitting the cell size s' jumps to s at time t with a given rate $W(s|s';t)$. Under this assumption, Eq. (3) can be written as

$$\begin{aligned}\frac{\partial}{\partial t}p(s|s_0;t) = &-\frac{\partial}{\partial s}[g(s,t)p(s|s_0;t)] \\ &+ \int ds'[W(s|s';t)p(s|s_0;t) \\ &- W(s'|s;t)p(s|s_0;t)].\end{aligned} \tag{5}$$

The case of perfect symmetric splitting ($s' = 2s$) corresponds to the selection rule:

$$W(s|s';t) = 2\delta(2s - s')h(s,s'). \tag{6}$$

Some studies have explored the particular case where $h(s,s') = h(s') = k_d s'$, i.e., the splitting rate depending only on the size just before the division, with k_d being a constant and discarding the dependence on the size after the division [17,19,20]. This assumption results in:

$$\frac{\partial p}{\partial t}(s;t) = -\frac{\partial(g(s)p(s;t))}{\partial s} - (k_d s)p(s;t) + 2(k2s)p(2s;t), \tag{7}$$

which is also known as the population balance equation for a fixed population number [20,31–35]. Theoretical methods like moment closure have been used in past articles to solve (7) and some useful limits have been already studied [15,17,20]. In the following sections we will show a method that we developed to solve this equation.

B. The Chapman-Kolmogorov equation including division events

Some instabilities observed when solving (7) using the moment closure approximation [20] can be traced to the nonlocality of the operator (6). To overcome these nonlocalities, we propose to reparametrize the size distribution considering an additional variable: the number of divisions $n \in \{0, 1, 2, \cdots\}$ [19]. In this case, the probability distribution is now $p(s,n;t)$ with transition rates satisfying:

$$W(s,n|s',n';t) = 2\delta(2s - s')\delta_{n,n'+1}h(s,s'), \tag{8}$$

with $\delta_{i,j}$, the Kronecker delta.

This means that after division not only is the size halved but the number of divisions n is increased by one unit. In the particular case where $h(s,s') = k_d s'$, the associated CKE is as follows:

$$\begin{aligned}\frac{\partial}{\partial t}p(s,n|x_0;t) &= \underbrace{-\frac{\partial}{\partial s}[g(s)p(s,n|x_0;t)]}_{\text{Drift by growth}} \\ &+ \underbrace{[2(k_d 2s)p(2s,n-1|x_0;t) - (k_d s)p(s,n|x_0;t)]}_{\text{Jumps by divisions}},\end{aligned} \tag{9}$$

where $x_0 = (s_0, n_0)$.

The inclusion of the new variable n breaks the nonlocality of the operator $W(s|s',t)$ that makes (5) hard to solve. Instead, $W(s,n|s',n-1,t)$ performs jumps between independent subspaces which can be merged together later using marginal sums.

Using this new variable n, exponential growth, and $s(0) = s_0$, Eq. (9) has closed solutions of the form

$$p(s, n; t) = \delta[s - s(n, t)]P_n(t), \tag{10}$$

where $P_n(t)$ is the probability of having divided n times at time t. We will present its associated equation later. $s(n, t)$ corresponds to the bacterial size after n divisions at a time t.

To explain how to solve for this $s(n, t)$, let us consider the size $s(1, t)$ at time t after one division. If t_1 is the time when division occurs, the size after that division was $s(1, t_1) = \frac{s_0 e^{\mu t_1}}{2}$ so, then the size any time $t > t_1$ is as follows:

$$s(1, t) = \frac{s_0 e^{\mu t_1}}{2} e^{\mu(t-t_1)}. \tag{11}$$

For a sequence of division times $0 < t_1 < t_2 < \ldots < t_{n-1} < t_n < t$, $s(n, t)$ satisfies:

$$\begin{aligned} s(n, t) &= s_0 \left[\prod_{i=1}^{n} \frac{e^{\mu(t_i - t_{i-1})}}{2}\right] e^{\mu(t-t_n)} \\ &= \frac{s_0}{2^n} \exp\left[\mu \sum_{i=1}^{n} (t_i - t_{i-1}) + \mu(t - t_n)\right] \\ &= \frac{s_0}{2^n} e^{\mu(t-t_0)} = \frac{s_0 e^{\mu t}}{2^n}, \end{aligned} \tag{12}$$

where we have used $t_0 = 0$ and the telescopic property of the sum.

Using this result and Eq. (10), Eq. (9) can be separated into the system of equations:

$$\begin{aligned} p(s; t) &= \sum_{n=0}^{\infty} p(s, n; t) = \sum_{n=0}^{\infty} \delta\left(s - \frac{s_0 e^{\mu t}}{2^n}\right) P_n(t) \\ \frac{dP_0}{dt} &= -k_d s_0 e^{\mu t} P_0 \\ &\vdots \\ \frac{dP_n}{dt} &= -\frac{k_d s_0 e^{\mu t}}{2^n} P_n + \frac{k_d s_0 e^{\mu t}}{2^{n-1}} P_{n-1} \\ &\vdots \end{aligned} \tag{13}$$

defining the dynamics of every $P_n(t)$.

C. The division strategy

In most phenomenological approaches to bacterial division [11,12,36], it is described by the relationship between the added cell size and the cell size at birth. This relationship is known as the *division strategy* [11,16] and in this section, we will explore how to obtain the division strategy from the solution of (13).

Focusing on the jump process between the state $n - 1$ to n (one division), we can change the space $n \in 0, 1, 2, \cdots$ to $n \in \{0, 1\}$ and truncate (13) to:

$$\begin{aligned} \frac{dP_0}{dt} &= -h(s)P_0 \\ \frac{dP_1}{dt} &= h(s)P_0, \end{aligned} \tag{14}$$

where a general size-dependent splitting rate function $h(s)$ can be used. This system can be integrated under the initial conditions $P_0(0) = 1$ and $P_1(0) = 0$. Thus, the probability $P_1(t)$—or to simplify notation, $P(t)$—that the cell divides in the time interval $(0, t)$ evolves according to

$$P(t) = 1 - \exp\left\{-\int_0^t h[s(t')]dt'\right\}. \tag{15}$$

In the particular case where $h(s)$ is proportional to the size, $h(s) = k_d s$, and assuming exponential growth as well, the integration on time can be done using the implicit formula

$$h[s(t)] = k_d s(t) = k_d s_0 e^{\mu t}. \tag{16}$$

Once $P(t)$ is obtained, the probability density function $\rho(t)$ for the time of division can be obtained as

$$\rho(t) = \frac{dP(t)}{dt}. \tag{17}$$

A transformation of variables allows us to get the distribution of sizes at division $\rho(s_d)$:

$$\rho(s_d) = \rho[t(s_d)]\frac{dt}{ds_d}, \tag{18}$$

where, if we assume exponential growth $t(s_d) = \frac{1}{\mu}\ln(\frac{s_d}{s_0})$, then $\frac{dt}{ds_d} = \frac{1}{\mu s_d}$. Using this $\rho(s_d)$ one can calculate the mean size at division by integrating:

$$\langle s_d \rangle = \int_{s_b}^{\infty} s_d \rho(s_d) ds_d. \tag{19}$$

Hence, we can calculate the mean added size per cell cycle $\langle \Delta \rangle = \langle s_d \rangle - s_b$ as a function of the size at birth s_b. This relationship defines the division strategy.

D. Multistep division for a single division

More generally, division does not have to correspond to a single jump process. Instead, division can occur once bacteria have reached some goal number of steps M. If the occurrence rate of these steps is proportional to the cell size s by a constant k_d, then the probability $P_m(t)$ of performing $m < M$ steps at time t can be modeled according to:

$$\begin{aligned} \frac{dP_0}{dt} &= -k_d s(t) P_0 \\ &\vdots \\ \frac{dP_m}{dt} &= k_d s(t) P_{m-1} - k_d s(t) P_m \\ &\vdots \\ \frac{dP_M}{dt} &= k_d s(t) P_{M-1}, \end{aligned} \tag{20}$$

where P_M is the probability of reaching the target steps M or, equivalently, the probability of a division event to occur. Once the division event happens, the process is reset to zero steps and size is halved.

Using this $P_M(t)$ and growth as described by (4) and following (18), the probability density $\rho(s_d|s_b)$ of size at division

s_d given the size at birth s_b in a cell cycle satisfies [16]:

$$\rho(s_d|s_b) = \left(\frac{k_d}{\mu}\right)^M \frac{(s_d - s_b)^{(M-1)}}{(M-1)!} \exp\left[-\frac{k_d}{\mu}(s_d - s_b)\right]. \tag{21}$$

Defining the added size before division as $\Delta = s_d - s_b$, we observe that $\langle\Delta\rangle = \langle s_d\rangle - s_b$ is independent of the size at birth s_b and depends on the growth rate μ, the target steps M and the step occurrence rate k_d:

$$\langle\Delta\rangle = M\frac{\mu}{k_d}. \tag{22}$$

The master equation (20) can be generalized to consider multiple division events in a similar way to Eq. (13). We will present this generalization in the following section.

E. Solution of the CKE including multiple divisions

Using a similar procedure as (13) but now with the additional variable m, the probability of the cell size being s, having performed m division steps and n divisions at time t, can be written as:

$$p(s, n, m; t) = \delta[s - s(n, t)]P_{m,n}. \tag{23}$$

The cell size $s(n, t)$ follows Eq. (12). The probability $P_{m,n}(t)$ of a cell having performed m division steps and n division events at time t can be obtained through the master equation system

$$\begin{aligned}
\frac{dP_{0,0}}{dt} &= -k_d s_0 e^{\mu t} P_{0,0} \\
\frac{dP_{1,0}}{dt} &= k_d s_0 e^{\mu t} P_{0,0} - k_d s_0 e^{\mu t} P_{1,0} \\
&\vdots \\
\frac{dP_{m,n}}{dt} &= \frac{s_0 e^{\mu t}}{2^n} P_{m-1,n} - \frac{s_0 e^{\mu t}}{2^n} P_{m,n} \\
&\vdots \\
\frac{dP_{M-1,n}}{dt} &= k_d \frac{s_0 e^{\mu t}}{2^n} P_{M-2,n} - k_d \frac{s_0 e^{\mu t}}{2^n} P_{M-1,n} \\
\frac{dP_{0,n+1}}{dt} &= k_d \frac{s_0 e^{\mu t}}{2^n} P_{M-1,n} - k_d \frac{s_0 e^{\mu t}}{2^{n+1}} P_{0,n+1} \\
&\vdots\ ,
\end{aligned} \tag{24}$$

where we include the selection rule defining the divisions as jumps between states $(M-1, n-1)$ to $(0, n)$ and the division steps as jumps between states (m, n) to $(m+1, n)$. These jumps happen at rate $h = k_d s(n, t)$ with $s(n, t)$ following Eq. (12).

The solution to (24) can be obtained by different methods. Analytically [19], one can start from the initial conditions

$$P_{m,n}(t = 0) = \delta_{n,0}\delta_{m,0}. \tag{25}$$

Hence, $P_{m,n}(t)$ can be obtained knowing $P_{m-1,n}(t)$ with $m \in 1, \ldots, M-1$, and $P_{0,n}(t)$ can be estimated from $P_{M-1,n-1}(t)$. Both using the closed recurrence expression:

$$\begin{aligned}
P_{m,n}(t) &= \frac{k_d s_0}{2^n} \exp\left[-\frac{k_d s_0}{\mu 2^n} e^{\mu t}\right] \int_0^t K_n(t') P_{m-1,n}(t') dt' \\
P_{0,n}(t) &= \frac{k_d s_0}{2^{n-1}} \exp\left[-\frac{k_d s_0}{\mu 2^n} e^{\mu t}\right] \int_0^t K_n(t') P_{M=1,n-1}(t') dt' \\
&\text{with} \\
K_n(\tau) &= \exp\left[\mu\tau + \frac{k_d s_0}{\mu 2^n} e^{\mu\tau}\right] \\
P_{0,0}(t) &= \exp\left[-\frac{k_d s_0}{\mu}(e^{\mu t} - 1)\right].
\end{aligned} \tag{26}$$

Explicit resulting expressions have length increasing with m becoming intractable in practice. To solve (24), we recommend the use of well-behaved numerical methods implemented in past studies [18] that are going to be presented in the next section.

III. NUMERICAL ESTIMATION OF SIZE DYNAMICS

A. The finite-state projection algorithm

In general, in Eq. (24) the number of possible division steps $m \in \{0, 1, \ldots, M-1\}$ is finite but the number of possible divisions $n \in \{0, 1, \cdots\}$ is infinite. This thwarts the complete solution of (24) using methods like Matrix exponential. As we explained before [19], this infinite set can be projected into a finite set using the well-known finite state projection algorithm [37]. Using this approach, the number of equations in (24) are truncated up to a maximum N of divisions, allowing common methods for solving these finite systems to be used to determine size dynamics during infinitesimal periods of time.

From $P_{m,n}(t)$, the size distribution $\rho(s|s_0)$ given the starting size s_0, and the mean size $\langle s\rangle$ and variance $\mathrm{var}(s) = \langle s^2\rangle - \langle s\rangle^2$ can be obtained from the equations:

$$\begin{aligned}
\rho(s|s_0) &= \sum_{n=0}^{N} \delta\left(s - s_0\frac{e^{\mu t}}{2^n}\right) P_n \\
\langle s\rangle &= \sum_{n=0}^{N} s_0 \frac{e^{\mu t}}{2^n} P_n \\
\mathrm{var}(s) &= \sum_{n=0}^{N} \left[\left(s_0\frac{e^{\mu t}}{2^n}\right)^2 - \langle s\rangle^2\right] P_n,
\end{aligned} \tag{27}$$

with $P_n = \sum_{m=0}^{M} P_{m,n}$.

The computation of these moments was done assuming that all cells began at an initial size $s(0) = s_0$, that is, $\rho(s_0) = \delta[s_0 - s(0)]$. However, if a general density function $\rho(s_0)$ for the initial sizes is considered, then the size distribution $\rho(s)$ is a convolution of solutions of (27):

$$\rho(s) = \int \rho(s|s_0)\rho(s_0) ds_0. \tag{28}$$

Until now, we have obtained expressions for the size distribution $\rho(s; t)$ at an arbitrary time t. In some cases, it might be of interest to simulate single-cell trajectories. To do that, we have to develop an algorithm to obtain the division times as

random variables distributed following Eq. (17). This procedure is explored in the following section.

IV. STOCHASTIC SIMULATION OF SIZE DYNAMICS

Consider the single-step process described by (14). While Eqs. (14) were written for modeling the division as a single-step process, in general these equations are also valid for the occurrence of a division step. Setting explicitly the propensity $h = k_d s$, the equations describing the occurrence of a division step are now:

$$\frac{dP_0}{dt} = -k_d s_0\, e^{\mu t}\, P_0 \quad \frac{dP_1}{dt} = k_d s_0 e^{\mu t} P_0. \tag{29}$$

If $P_0(0) = 1$ and $P_1(0) = 0$, then $P_1(t)$, or simply $P(t)$, has the explicit solution:

$$\begin{aligned} P(t) &= 1 - \exp\left[-\int_0^t k_d s(t')dt'\right] \\ &= 1 - \exp\left[-s_0\frac{k_d}{\mu}(e^{\mu t} - 1)\right], \end{aligned} \tag{30}$$

while the associated probability density function is as follows:

$$\rho(t) = \frac{dP(t)}{dt} = s_0\frac{k_d}{\mu}\exp\left[\mu t - s_0\frac{k_d}{\mu}(e^{\mu t} - 1)\right]. \tag{31}$$

The main idea behind the stochastic simulation algorithm is to generate random time events τ_s distributed as (31). Following Gillespie's method [38], we generate a random number r uniformly distributed in the interval (0,1) and from the cumulative function (30), τ_s is obtained by matching $P(t)$ and r and solving for t:

$$\tau_s = \frac{1}{\mu}\ln\left[1 - \frac{\mu}{s_0 k_d}\ln(r)\right], \tag{32}$$

where we take advantage of the fact that $1 - r$ is distributed as r. This τ_s is the time to the occurrence of the next division step.

V. INCLUDING ADDITIONAL ASPECTS OF CELL DIVISION

Two assumptions behind (12) are that after each division the cell size is halved perfectly and that the growth rate is a constant equal for all cells. However, this is not the case in actual cell splitting. Two notable sources of stochastic fluctuations are variations in both partitioning of volume and cellular components among daughter cells [23,39] and random fluctuations in the cell growth rate [40,41]. In this section we will explore how to include these sources of noise as well as other important properties of bacterial division such as division strategies different form the *adder*, and we explore the size convergence to reach homeostasis, an important property found experimentally [14].

A. Nonsymmetric splitting

Stochastic fluctuations in the septum position are observed experimentally. For some growth conditions this noise can be as high as 5% [24,42–44].

Considering again the size at time t after one division, if the division occurred at time $t_1 < t$ and if the size is not perfectly halved but multiplied by a random variable b_1 (also known as the division ratio) centered on 0.5, then the size at time t is now

$$s(1,t) = s_0 e^{\mu(t_1 - t_0)} b_1 e^{\mu(t - t_1)}. \tag{33}$$

If the sequence of division ratios $\{b_1, b_2, \cdots, b_n\}$ is known, then the size at time t after n divisions is given by

$$s(n,t) = s_0 e^{\mu t}\prod_{k=1}^{n} b_k. \tag{34}$$

Numerically, b_k can be approximated by a beta distributed variable centered on 0.5 with a variance fitted from experiments [24].

B. Cell-to-cell variability in growth rate

Another important stochastic variable is the cell-to-cell variability in growth rates [25,41]. This variability can be as high as 10% [3]. We assume that after a division, a new growth rate μ_k is chosen randomly from a distribution centered on $\langle\mu\rangle$ and cell grows during that cycle with rate μ_k. This ignores possible mother-daughter correlation in growth rates, which could be important [24,45], as well as fluctuations in the growth rate of a single cell within one generation. These considerations are not taken into account for simplicity.

With symmetric splitting, the size at time t after n divisions is now:

$$s(n,t) = \frac{s_0}{2^n}\left[\prod_{k=0}^{n-1}\exp[\mu_k(t_{k+1} - t_k)]\right]\exp[\mu_n(t - t_n)]. \tag{35}$$

Numerically, we modeled these μ_k as a gamma distributed variable centered on the mean growth rate $\langle\mu\rangle$, with the experimentally observed variance and no correlation with past cycles.

C. A general CKE including additional sources of noise

A general CKE assuming exponential growth and a growth rate distribution $\rho(\mu)$ can be modeled by [17]:

$$\begin{aligned} \frac{\partial p(s;t)}{\partial t} &= -\int\left[\frac{\partial}{\partial s}(\mu s p(s;t))\right]\rho(\mu)d\mu \\ &\quad + \int h(s,s')p(s';t)ds' - h(s)p(s;t). \end{aligned} \tag{36}$$

The division rate $h(s,s')$ is in general dependent on hidden variables (like the number of division steps). So its dependence with the size could not be easy to parametrize. Some studies have estimated this rate, at least, numerically for some cases [46–48], others include explicitly the division steps [17]. In the case of single-step division, this rate can be written as $h(s,s') = k_d s' \rho(s,s')$ with $\int \rho(s,s')ds' = \rho(s)$, where $\rho(s)$ is the distribution of size at birth. Nonsymmetric division can also be considered within $\rho(s,s')$. $h(s)$ in the last term is obtained from $h(s) = \int h(s'|s)ds'$. We do not yet have a closed solution to (36), but some useful limits have been already estimated [17].

D. Encompassing different division strategies

Depending on the mapping $s_d = f(s_b)$, or as described traditionally, on the relationship between added size $\Delta = s_d - s_b$ and s_b, three basic division strategies have been defined for exponentially growing bacteria: the *timer*, *adder*, and *sizer* strategies [36]. They can be distinguished by differences in the slope of Δ vs s_b: For the timer this slope is $+1$, whereas it is -1 for the sizer and 0 for the adder. The adder strategy, observed for instance in *E. coli* and *Bacillus subtilis* [3], is considered the most common strategy in bacteria. In some bacterial populations, however, division strategies with intermediate slopes for Δ vs s_b have also been observed [16,36]. This has led to the definition of the *timerlike* strategy for slopes between 0 and 1, and of the *sizerlike* strategy for slopes between -1 and 0.

These deviations from the adder can be obtained from our framework if the step rate (h) is not proportional to the size but to a power (λ) of the size [16]. That is,

$$h = k_d s^{\lambda}. \tag{37}$$

A multistep process similar to that described by (24) can also be proposed in this case. If division is triggered by the occurrence of M steps happening at rate (37), then the distribution of size at division s_d given the size at birth s_b is [16]:

$$\rho(s_d|s_b) = \left(\frac{k_d s_d^{\lambda-1}}{\mu}\right) \exp\left[-\frac{k_d}{\mu\lambda}(s_d^{\lambda} - s_b^{\lambda})\right] \times \frac{\left[\frac{k_d}{\mu\lambda}(s_d^{\lambda} - s_b^{\lambda})\right]^{M-1}}{(M-1)!}. \tag{38}$$

The timer strategy is obtained if $\lambda \to 0$, the sizer strategy is obtained if $\lambda \to \infty$, and the adder is obtained when $\lambda = 1$.

Considering the nonlinear step rate given by Eq. (37) and using a similar method to (31), the general stochastic time is given by:

$$\tau_s(\lambda) = \frac{1}{\lambda\mu} \ln\left[1 - \frac{\lambda\mu}{k_d s_0^{\lambda}} \ln(r)\right]. \tag{39}$$

E. Mean cell size at birth

The main variables defining the mean cell size are the growth rate μ, the number of division steps M, and the division steps occurrence rate k_d. If an adder strategy is considered ($\lambda = 1$), then the mean added size $\langle\Delta\rangle$ follows the relationship (22).

Given the uncertainties about the nature of k_d, the inference of its actual value is not straightforward. For the adder, this k_d can be inferred from the mean added size using (22) and by observing that this $\langle\Delta\rangle$ is independent on the size at birth s_b. In other division strategies ($\lambda \neq 1$), $\langle\Delta\rangle$ is now a function of s_b. Now, the typical size as explained in past studies [16,20], $\overline{s_b}$, is the size at birth that is perfectly doubled by the division strategy:

$$\overline{s_b} = s_b : \langle s_d\rangle(s_b) = 2s_b. \tag{40}$$

In general, $\overline{s_b}$, is dependent on k_d, μ, and λ and is one of the variables that can be measured most easily if we assume that this $\overline{s_b}$ is actually the mean size at birth in a steadily growing cell population. Other variables such as k_d can be estimated from this $\overline{s_b}$ using (40) and root-finding algorithms.

F. Discrete translation invariance

To illustrate the dynamics of the probability of having divided n times at time t, we present in Fig. 1 time trends of some $P_n(t)$s for different λs and Ms with initial condition $P_{n,m}(0) = \delta_{n,0}\delta_{m,0}$.

A numerical analysis of the behavior in Fig. 1 allows us to find that, in the limit of $t \to \infty$, the distribution of P_ns satisfies

$$\lim_{n\to\infty} \|P_n(t) - P_{n+1}(t+\tau)\| = 0, \tag{41}$$

with $\tau = \frac{\ln(2)}{\mu}$ being the doubling time.

This limit, whose convergence was estimated numerically in Appendix A, implies asymptotic invariance of the system (explicitly of P_n) under translation on, simultaneously, $n \to n+1$ and $t \to t+\tau$. Since $\frac{s_b e^{\mu t}}{2^n}$ also satisfies this invariance, we expect $\rho(s|t, s_b)$ to show periodic properties in the limit $t \to \infty$. This periodicity was already discussed in some theoretical papers [49–51].

VI. ILLUSTRATING EXAMPLES

To explore the effects of the above-mentioned additional sources of noise on the periodical properties of bacterial division, we used our formalism to test three different scenarios for size dynamics:

(i) The size dynamics considering only stochastic division times following (31). This can be done solving (26).

(ii) The size dynamics considering a distribution of initial sizes at $t = 0$. This can be obtained numerically by convolution of the initial size (28).

(iii) The size dynamics considering two additional sources of noise: noise in splitting and noise in growth rate. This can be explored using stochastic simulations.

Figure 2(a) shows the first case where the mean size dynamics are obtained from a simulation of 5000 cells, all of them with the same starting size and beginning with zero division steps or equivalently, starting from their most recent division. We assumed that they have the same growth rate and are split perfectly evenly. The simulation was done using stochastic times (32) and numerical estimation was done by solving the master equation (24). Both approaches show perfect adjustment to each other.

Ten examples of individual cell trajectories were plotted in the background to show how variable the distributions are. The dynamics of this variability, quantified by the coefficient of variation $C_v^2(s) = \frac{\mathrm{var}(s)}{\langle s\rangle^2}$, is also shown in Fig. 2(e). As our main observation, we highlight the oscillations in both $\langle s\rangle$ and $C_v^2(s)$ with period equal to $\tau = \frac{\ln(2)}{\mu}$, the doubling time. The oscillations in the $C_v^2(s)$ present their peaks just when bacteria are dividing on average and their valleys when bacteria are growing. The dynamics of the size distribution can be seen in Supplemental video 1 [52].

Figure 2(b) illustrates the second case, where the mean dynamics corresponds to cells with an initial distribution with finite noise [$C_v^2(s, t = 0) = 0.02$]. This distribution was assumed to be a gamma distribution since it is well defined

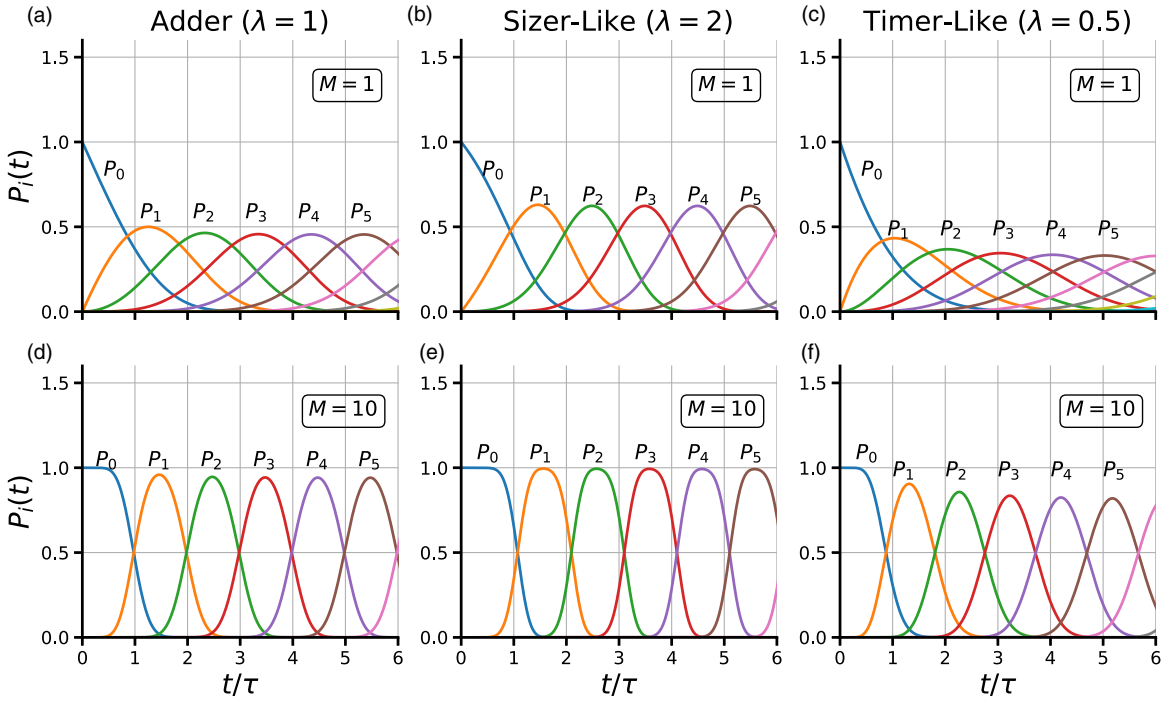

FIG. 1. Time dynamics of the first P_n for different division strategies and division steps (M) with $\rho(s_b) = \delta(s_b - \overline{s_b})$.

from its mean size and the $C_v^2(s)$. Simulations, on the other hand, were modified by using random initial sizes and numerical estimation was done by performing the convolution (28) and approximating the integral by a numerical Riemann sum. Dynamics on cell-size variability are also presented in Fig. 2(f). Oscillations were again found in both the mean and the variance but with less amplitude than in the first case. The dynamics of this distribution appear in Supplemental video 2 [52].

Figure 2(c) presents the third scenario with the assumption that bacteria do not split perfectly in half but according to a beta distributed independent stochastic variable centered on 0.5 and with a given noise $C_v^2 = 0.002$. Growth rate could be considered stochastic as well with variability set to $C_v^2 = 0.02$. The dynamics of the mean size [Fig. 1(c)] and its C_v^2 [Fig. 1(h)] are presented. We plotted trajectories for ten individual cells in the background of Fig. 2(c) to give a sense of the distribution. Since these noises are not considered in

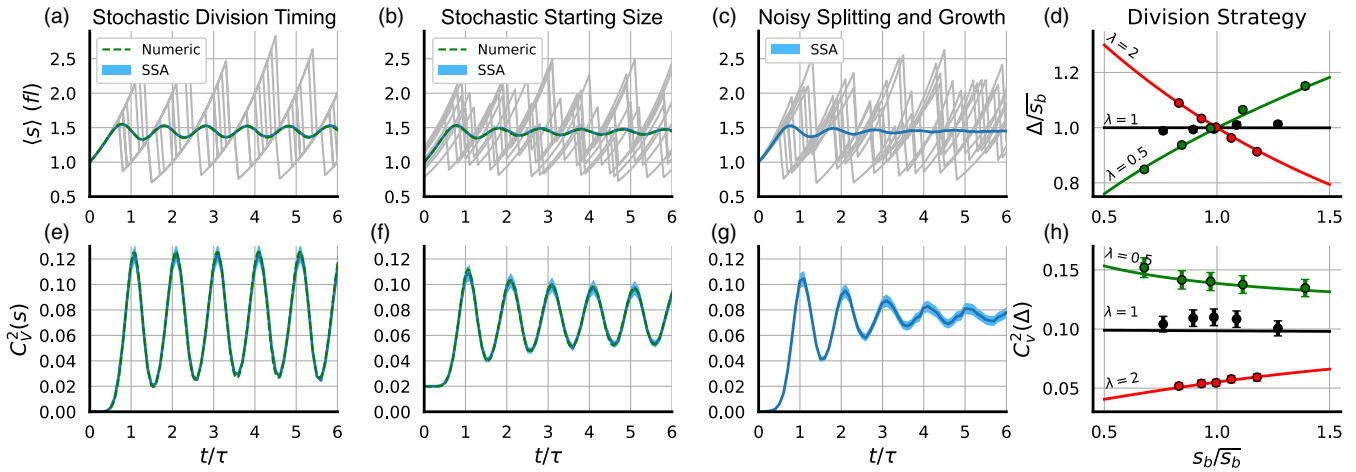

FIG. 2. Dynamics of the moments of the cell-size distribution. (a) Mean cell size $\langle s \rangle$ with some single-cell trajectories in gray and (e) its noise $C_v^2(s)$ as a function of time considering only stochastic division timing. (b) Mean cell size with some single-cell trajectories in gray and (f) its noise as a function of time considering both stochastic division timing and an initial size distribution with finite variance. (c) Mean cell size with some single-cell trajectories in gray and (g) its noise as a function of time considering stochastic division and noise in cell-to-cell growth rate and septal position. (d) Mean added size Δ vs the size at birth s_b and (h) the fluctuations $C_v^2(\Delta)$ vs s_b for different division strategies. Timerlike ($\lambda = 0.5$), adder ($\lambda = 1$) and sizerlike ($\lambda = 2$). Simulations (dots) and numerical estimations (lines) are shown. $M = 10$ division steps were considered in all cases.

Eq. (24), the same numerical approach is not feasible. The distribution dynamics can be seen in Supplementary video 3 [52].

We also explore the division strategy using both simulations and numerical estimations. Data from stochastic simulations can be obtained using the stochastic division times (39) and exponential growth (4) while the trends in added size and its variability can be obtained from the distribution of size at division (38), both being dependent on the exponent λ. In Fig. 2(d). we present the mean added size Δ as a function of the mean size at birth s_b for three different values of λ. These values were chosen to represent three of the most important division strategies: timerlike ($0 < \lambda < 1$, where we choose $\lambda = 0.5$) with its characteristic positive slope on Δ vs s_b, adder ($\lambda = 1$) with no correlation between Δ and s_b and sizerlike ($1 < \lambda < \infty$, where we choose $\lambda = 2$) with a negative slope in Δ vs s_b. Fluctuations over the trends are also shown in Fig. 2(h). where it can be seen that sizerlike shows positive correlation in $C_v^2(\Delta)$ vs s_b, adder strategy shows no-correlation and timerlike shows a negative correlation.

To better understand the properties of the robust oscillations on the dynamics of the central moments presented in Fig. 2(a) and Fig. 2(b), we studied the autocorrelation function of the size. This autocorrelation $\gamma(t')$ is defined through the formula:

$$\gamma(t') = \lim_{T\to\infty} \frac{1}{T} \times \int_0^T \frac{\langle\{[s(t) - \langle s(t)\rangle][s(t+t') - \langle s(t+t')\rangle]\}\rangle}{\sigma(t)\sigma(t+t')} dt, \tag{42}$$

with $\sigma(t)$ being the standard deviation of the size at time t and $\langle x\rangle$ is the mean value of the random variable x

In Fig. 3(a) we show how the autocorrelation dynamics change as a function of time. We present four different cases: first, a single division step [19]. This autocorrelation decays exponentially to zero. By increasing the division steps, for instance to 10 steps, oscillations appear around a decaying trend. For a division that is almost deterministic, for instance 50 steps, these oscillations have higher amplitude around zero. When noise on both growth rate and septum position is considered, these oscillations are damped in the same way found in size dynamics, converging to zero. This asymptotic decorrelation lets the distribution reach a stationary distribution with fixed moments which is presented in Fig. 3(b) for $M = 10$ and the noises explained above.

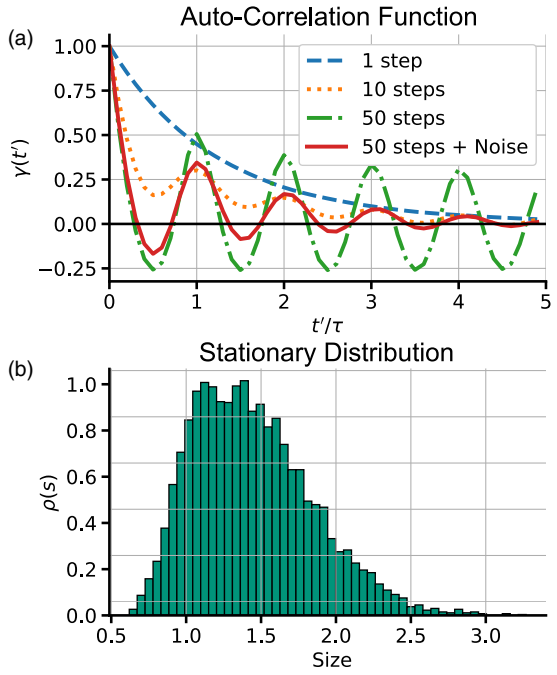

FIG. 3. (a) Cell-size autocorrelation $\gamma(t')$ for different time periods t' for four different division conditions: one division step (dashed blue line), 10 division steps (dotted orange line), 50 division steps (green dash-dotted line), and 50 division steps including noise in growth rate and septum position (red continuous line). (b) Simulation of stationary state of the histogram of bacterial size with all the noise sources considered in Fig. 2(c).

VII. DISCUSSION

In this article we summarize and extend previous results to construct a theoretical framework based on the Chapman-Kolmogorov equation to model the stochastic dynamics of the cell size for a population of growing cells. While we limited ourselves to a population of constant number, such as what you have in a turbidostat or mother-machine experiment, the approach can be extended to cover a growing population. Unfortunately, this exponential growth in the number of cells imposes practical constrains on the type of stochastic simulations we used for the more realistic cases.

Our framework can be used for obtaining the size distribution dynamics, as well as the distribution of division times, and it allows for the inclusion of sources of noise such as variations in division volumes and cell-to-cell growth rate differences [24]. Most importantly, the different splitting rates that result in the various division strategies found in *E. coli*: Timerlike, adder, and sizerlike [11,36] can be incorporated quite naturally.

As an example of our framework's use, we consider cells starting from their last division. We predict oscillations in both the mean size $\langle s\rangle$ and noise $C_v^2(s)$, shown in Fig. 2. What is noteworthy is that these oscillations are robust to some sources of noise but not others. When only stochasticity on division times is considered, these oscillations are maintained over an arbitrary long period of time. They lose amplitude when an initial size distribution is considered, and rapid damping occurs if other sources of noise like the cell-to-cell growth rate variability and septum position are added.

The robustness of the oscillations can be understood as result of the asymptotic periodic properties of the probability P_n of having n divisions at time n. These probabilities are invariant under the simultaneous transformation $n \to n+1$ and $t \to t+\tau$. The way to damp these oscillations is breaking that symmetry. The inclusion of these additional sources of noise is a simple way to do that but other way is to consider cases with different symmetries for instance other forms of division and growth rates. See, for instance, the damped oscillations in bacteria that grow linearly having either constant or

size-dependent splitting rate, using similar approach to Ref. [20] but including division steps, with no additional sources of noise in Appendix B.

The properties found in size dynamics can be also obtained using the classical discrete stochastic maps approach [11,12]. A clear correspondence between DSM and our model can be found when the adder strategy is considered. In this case, the stochastic map between size at birth s_b and size at division is

$$s_d = s_b + \Delta + \epsilon, \tag{43}$$

with ϵ being an independent random variable with zero mean and a distribution fitted from experiments. If exponential growth is considered, then the cell-cycle duration τ_d, as random variable, can be obtained from (43):

$$\tau_d = \frac{1}{\mu} \ln\left[1 + \frac{\Delta}{s_b}\left(1 + \frac{\epsilon}{\Delta}\right)\right], \tag{44}$$

where, using (22), some analogy to (32) can be found. Using these times with parameters fitted from the data, similar oscillations in both size trends and autocorrelation can be obtained.

The main difference with DSMs is found where deviations from the adder are considered. Using the CRMs, the fluctuations (ϵ) in the division strategy (43) will depend on the size at birth, unlike in the DSM where these fluctuations are not related to any other variable. Some preliminary observations on the dependence of the fluctuations on added size with the size at birth in sizerlike division in *E. coli* have been reported [16,53] but further experiments are needed.

To better understand how each kind of noise affects the size-distribution dynamics, we studied the dynamics of central moments in some extreme cases (see Appendix C). We observe that growth rate noise results in a similar mean size while the noise in splitting position can make the mean smaller than in the noiseless case. Experimentally, the observed noises are so small that we could not discriminate between these effects. To observe how these noises affect the damping of the autocorrelation function, we measured the peak of the Fourier transform of this function while varying the noise. We found that using this measure of the damping, the effects of both noises are equivalent (see Appendix C).

Including cell-size stochasticity in models of gene expression can be an important tool to understand the origin of the fluctuations in molecule concentration. Some efforts have already been done to understand these effects in simple regulatory networks [54–57] but our formalism can expand this to more complex gene regulatory architectures.

As we learn more about the changes in division strategies that occur when environmental conditions change, our framework should facilitate the theoretical modeling of such processes, allowing their description as simple changes of the splitting rate functions. This in turn should guide the search for the specific biochemical mechanisms, as well as allowing the construction of ever more realistic computational models.

ACKNOWLEDGMENTS

C.V.-G. Acknowledges Colombian Ministry of ICT (MinTIC), Data Sanbox Initiative. C.N. Acknowledges COLCIENCIAS convocatoria 647 para doctorados nacionales for the financial support.

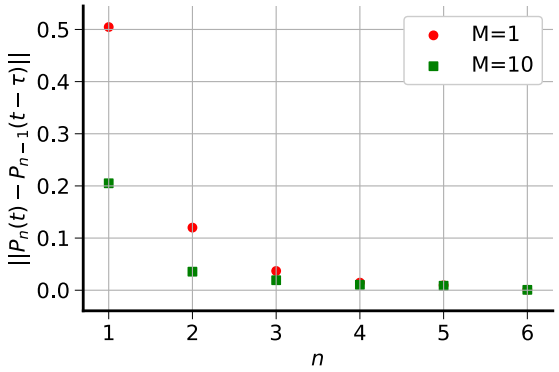

FIG. 4. Distance between the probabilities $P_n(t)$ and $P_{n-1}(t-\tau)$ for two different division steps (red dots: $M = 1$) (green squares: $M = 10$).

APPENDIX A: THE ASYMPTOTIC PERIODICITY OF THE SYSTEM

To check the property (41), we calculate numerically the distance between the probabilities $P_n(t)$ and $P_{n-1}(t-\tau)$ with τ being the doubling time $\tau = \frac{\ln(2)}{\mu}$, using the expression:

$$\|P_n(t) - P_{n-1}(t-\tau)\| = \int |P_n(t) - P_{n-1}(t-\tau)|dt, \tag{A1}$$

the results are presented in Fig. 4 where we can check how this distance decays asymptotically to zero as n increases.

APPENDIX B: SIZE DYNAMICS FOR DIFFERENT GROWTH CONDITIONS AND DIVISION RATES

Past studies suggested that the periodicity under translations in τ and n is an exclusive property of exponential growth [49]. Thus, if other growth conditions are considered, then the symmetry under time translations is broken and robust oscillations are not expected.

We simulated the size dynamics of different possible growth and division rates in a similar way to past studies [20]. Thus, we define the growth law as (2), where exponential growth is defined as $g(s,t) = \mu s$ and the linear growth is given by $g(s,t) = \mu$ with μ being a constant. On the other hand, the division rate is defined by the function h as (6). In Fig. 5, we compare two division rates for linear growth, one of these is $h = k_d$ and the other is $h = k_d s$ with k a constant. These rates define the occurrence of a given division step. In Fig. 5 we considered $M = 10$ steps to trigger the division.

In Fig. 5(a) we present the dynamics of the mean cell size $\langle s \rangle$ as a function of time with some single trajectories presented in the background (gray lines). In Fig. 5(c) we present its noise $C_v^2(s)$ as a function of time for linear growth $g = \mu$ and constant division rate $h = k$. Figure 5(b) $\langle s \rangle$ vs t and Fig. 5(d) $C_v^2(s)$ vs t both for a linear growth $g = \mu$ and a division rate proportional to the cell size $h = k_d s$. Perfectly symmetric splitting and fixed growth rate are considered.

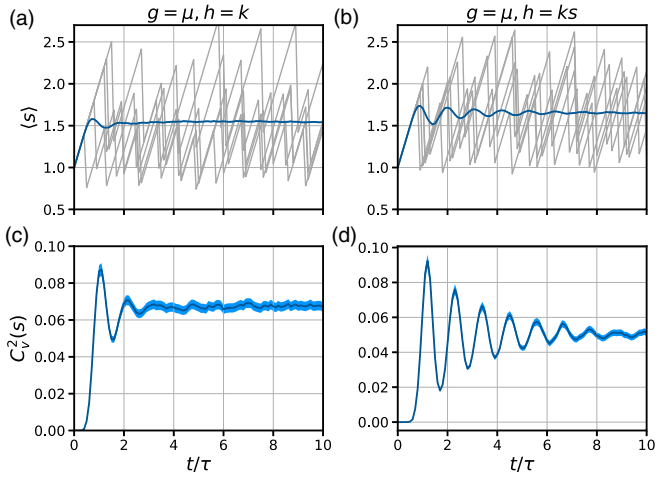

FIG. 5. Mean cell-size $\langle s \rangle$ and its noise $C_v^2(s)$ as a function of time for different growth and splitting rates similarly to [20]. (a) $\langle s \rangle$ vs t and (c) $C_v^2(s)$ vs t both for a linear growth $g = \mu$ and constant division rate $h = k$. (b) $\langle s \rangle$ vs t and (d) $C_v^2(s)$ vs t both for linear growth $g = \mu$ and a division rate proportional to the cell-size $h = k_d s$. $\tau = 1mu$. In both cases, 10 division steps and 5000 cells were considered.

APPENDIX C: THE EFFECT OF NOISE IN SPLITTING AND NOISE IN THE GROWTH RATE

In the main text, we showed how two kinds of noise: The cell-to-cell variability in growth rate and stochastic variability in division ratio can damp the oscillations in both the central moments and the autocorrelation function.

To explain better the effect of each kind of noise in the division process, in Fig. 6(a), we present the dynamics of the mean (blue) and an example of a single-cell size-trajectory

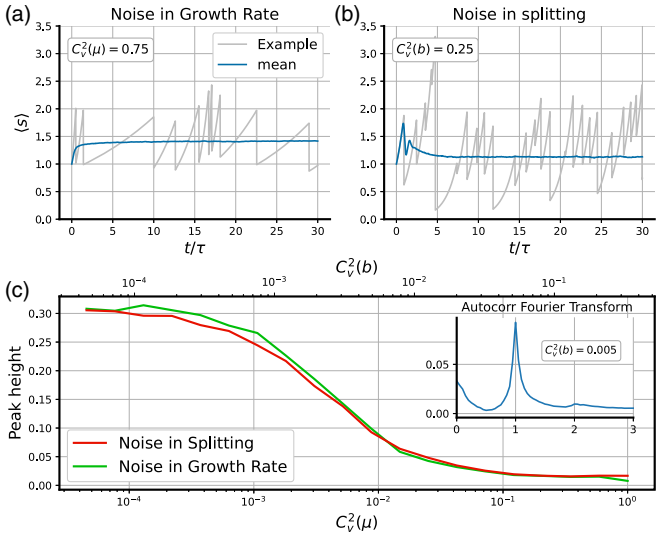

FIG. 6. (a) Size dynamics for the mean (blue) and a single trajectory (gray) with relatively high noise in growth rate. (b) Size dynamics for the mean (blue) and a single trajectory (gray) with relatively high noise in splitting position. (c) Effect of the noise in both the growth rate and the splitting position measured as the height of the peak of the Fourier transform of the autocorrelation function.

with a relatively high noise $[C_v^2(\mu) = 0.75]$ in the growth rate μ. As explained in the main text, during division, we select a growth rate for the next cycle as a random variable distributed following the gamma distribution with mean $\langle \mu \rangle$ and the above mentioned variability $C_v^2(\mu)$. The division rate k_d is selected proportional to the given μ such as the mean added size before division is fixed. Bacteria are perfectly halved during division. In order to reduce the noise in division timing, we choose $M = 50$ division steps making the division almost deterministic in time. As observed in Fig. 2, the mean size also goes to $\approx 1.416 \frac{\mu}{Mk_d}$ as $t \to \infty$.

To study the noise in splitting position, we used a similar approach. In Fig. 6(b), we present the dynamics of the mean (blue) and an example of a single-cell size-trajectory with a relatively high noise $[C_v^2(b) = 0.25]$ in the splitting ratio b. As explained in the main text, during division we select the splitting ratio as a random variable distributed following a beta distribution with mean 0.5 and the above mentioned $C_v^2(b)$. The size of the new cell after division is the size of the mother size times this splitting ratio. Both the division rate k_d and the growth rate μ are fixed for all the cells such that the mean added size before division is fixed and $M = 50$ division steps were considered. Unlike what is observed in Fig. 2, the mean size is altered reaching a steady-state value smaller than when considering only noise in growth rate. This can be due to the possibility of having very small bacteria, and since they take more time to reach the target division steps, these small bacteria are over-represented in the sampled population. A similar effect was also reported previously [20].

To understand better the effect of each kind of noise on the damping, we study the Fourier Transform of the autocorrelation function. As result of the oscillations, we expect a peak in the main harmonic corresponding to a period of one doubling time $\tau = \frac{\ln(2)}{\mu}$. As result of the damping, when increasing the noise in each variable, we expect that peak to become smaller. In Fig. 6(c), we present the height of this peak when changing the noise in each variable.

To explain the limits in each case, we observe that, in the way we modeled each random variable, there are some higher limits on the possible noise. For instance, in the noise in splitting, the widest possible distribution is the uniform distribution in the interval (0,1) which has a $C_v^2(b) = 1/3$. So, in the Fig. 6(c) we present this $C_v^2(b)$ along the interval $(10^{-5}, 1/3)$ in logarithmic scale trying to present variations relative to this maximum possible $C_v^2(b)$. Regarding the noise in growth rate, in order to have a distribution parametizable with the mean and the variance, we selected the gamma distribution for this variable. In the same sense, the widest kind of gamma distribution with a given mean $\langle \mu \rangle$ is the exponential distribution having $C_v^2(\mu) = 1$. We therefore present the peak height with the noise in growth rate relative to the noise of the exponential distribution.

When we compare the effect of each kind of noise in the peak of the Fourier transform of the autocorrelation function, we observe that both noises affect it in similar way when we compare them relatively to the highest achievable noise. So the conclusion of this approach is that both noises damp the oscillations in a similar way but they can alter the size distribution modifying the central moments dynamics differently.

[1] M. Wallden, D. Fange, E. G. Lundius, Ö. Baltekin, and J. Elf, The synchronization of replication and division cycles in individual e. coli cells, Cell **166**, 729 (2016).

[2] M. Campos, I. V. Surovtsev, S. Kato, A. Paintdakhi, B. Beltran, S. E. Ebmeier, and C. Jacobs-Wagner, A constant size extension drives bacterial cell size homeostasis, Cell **159**, 1433 (2014).

[3] S. Taheri-Araghi, S. Bradde, J. T. Sauls, N. S. Hill, P. A. Levin, J. Paulsson, M. Vergassola, and S. Jun, Cell-size control and homeostasis in bacteria, Curr. Biol. **25**, 385 (2015).

[4] J. B. Andersen, C. Sternberg, L. K. Poulsen, S. P. Bjørn, M. Givskov, and S. Molin, New unstable variants of green fluorescent protein for studies of transient gene expression in bacteria, Appl. Environ. Microbiol. **64**, 2240 (1998).

[5] C. Nieto-Acuña, J. C. Arias-Castro, C. Vargas-García, C. Sánchez, and J. M. Pedraza, Correlation between protein concentration and bacterial cell size can reveal mechanisms of gene expression, Phys. Biol. **17**, 045002 (2020).

[6] Y. Taniguchi, P. J. Choi, G.-W. Li, H. Chen, M. Babu, J. Hearn, A. Emili, and X. S. Xie, Quantifying e. coli proteome and transcriptome with single-molecule sensitivity in single cells, Science **329**, 533 (2010).

[7] D. F. Anderson and T. G. Kurtz, *Stochastic Analysis of Biochemical Systems* (Springer, Berlin, 2015).

[8] J. M. Raser and E. K. O'shea, Noise in gene expression: Origins, consequences, and control, Science **309**, 2010 (2005).

[9] M. P. Swaffer, D. Chandler-Brown, M. Langhinrichs, G. Marinov, W. Greenleaf, A. Kundaje, K. M. Schmoller, and J. M. Skotheim, Size-independent mrna synthesis and chromatin-based partitioning mechanisms generate and maintain constant amounts of protein per cell, bioRxiv 2020.08.28.272690 (2020), doi: 10.1101/2020.08.28.272690.

[10] W. J. Blake, G. Balázsi, M. A. Kohanski, F. J. Isaacs, K. F. Murphy, Y. Kuang, C. R. Cantor, D. R. Walt, and J. J. Collins, Phenotypic consequences of promoter-mediated transcriptional noise, Molec. Cell **24**, 853 (2006).

[11] P.-Y. Ho, J. Lin, and A. Amir, Modeling cell size regulation: From single-cell-level statistics to molecular mechanisms and population-level effects, Annu. Rev. Biophys. **47**, 251 (2018).

[12] Y. Tanouchi, A. Pai, H. Park, S. Huang, R. Stamatov, N. E. Buchler, and L. You, A noisy linear map underlies oscillations in cell size and gene expression in bacteria, Nature **523**, 357 (2015).

[13] C. W. Gardiner *et al.*, *Handbook of Stochastic Methods*, vol. 3. (Springer, Berlin, 1985).

[14] P. Wang, L. Robert, J. Pelletier, W. L. Dang, F. Taddei, A. Wright, and S. Jun, Robust growth of escherichia coli, Curr. Biol. **20**, 1099 (2010).

[15] M. Osella, E. Nugent, and M. C. Lagomarsino, Concerted control of escherichia coli cell division, Proc. Natl. Acad. Sci. USA **111**, 3431 (2014).

[16] C. Nieto, J. Arias-Castro, C. Sánchez, C. Vargas-García, and J. M. Pedraza, Unification of cell division control strategies through continuous rate models, Phys. Rev. E **101**, 022401 (2020).

[17] C. Jia, A. Singh, and R. Grima, Cell size distribution of lineage data: Analytic results and parameter inference, Iscience **24**, 102220 (2021).

[18] C. Blanco, C. Nieto, C. Vargas-Garcia, and J. M. Pedraza, Pyecolib: A python library for simulating e. coli stochastic size dynamics, bioRxiv 2020.09.29.319152 (2020), doi: 10.1101/2020.09.29.319152.

[19] C. A. Nieto-Acuna, C. A. Vargas-Garcia, A. Singh, and J. M. Pedraza, Efficient computation of stochastic cell-size transient dynamics, BMC Bioinf. **20**, 647 (2019).

[20] N. Totis, C. Nieto, A. Küper, C. Vargas-García, A. Singh, and S. Waldherr, A population-based approach to study the effects of growth and division rates on the dynamics of cell size statistics, IEEE Contr. Syst. Lett. **5**, 725 (2020).

[21] F. Si, G. Le Treut, J. T. Sauls, S. Vadia, P. A. Levin, and S. Jun, Mechanistic origin of cell-size control and homeostasis in bacteria, Curr. Biol. **29**, 1760 (2019).

[22] K. Sekar, R. Rusconi, J. T. Sauls, T. Fuhrer, E. Noor, J. Nguyen, V. I. Fernandez, M. F. Buffing, M. Berney, S. Jun *et al.*, Synthesis and degradation of ftsz quantitatively predict the first cell division in starved bacteria, Molec. Syst. Biol. **14**, e8623 (2018).

[23] A.-C. Chien, N. Hill, and P. Levin, Cell size control in bacteria, Curr. Biol. **22**, R340 (2012).

[24] S. Modi, C. A. Vargas-Garcia, K. R. Ghusinga, and A. Singh, Analysis of noise mechanisms in cell-size control, Biophys. J. **112**, 2408 (2017).

[25] D. J. Kiviet, P. Nghe, N. Walker, S. Boulineau, V. Sunderlikova, and S. J. Tans, Stochasticity of metabolism and growth at the single-cell level, Nature **514**, 376 (2014).

[26] J. Lin and A. Amir, From single-cell variability to population growth, Phys. Rev. E **101**, 012401 (2020).

[27] P. Thomas, Making sense of snapshot data: Ergodic principle for clonal cell populations, J. R. Soc. Interface **14**, 20170467 (2017).

[28] Y. Hu and T. Zhu, Cell growth and size homeostasis in silico, Biophys. J. **106**, 991 (2014).

[29] B. van Brunt, A. Almalki, T. Lynch, and A. Zaidi, On a cell division equation with a linear growth rate, ANZIAM J. **59**, 293 (2018).

[30] C. A. Vargas-Garcia, K. R. Ghusinga, and A. Singh, Cell size control and gene expression homeostasis in single-cells, Curr. Opin. Syst. Biol. **8**, 109 (2018).

[31] M. A. Henson, Dynamic modeling of microbial cell populations, Curr. Opin. Biotechnol. **14**, 460 (2003).

[32] D. Ramkrishna and M. R. Singh, Population balance modeling: Current status and future prospects, Annu. Rev. Chem. Biomol. Eng. **5**, 123 (2014).

[33] J. Held, T. Lorimer, F. Pomati, R. Stoop, and C. Albert, Second-order phase transition in phytoplankton trait dynamics, Chaos **30**, 053109 (2020).

[34] A. G. Fredrickson, D. Ramkrishna, and H. M. Tsuchiya, Statistics and dynamics of procaryotic cell populations, Math. Biosci. **1**, 327 (1967).

[35] J. W. Sinko and W. Streifer, A new model for age-size structure of a population, Ecology **48**, 910 (1967).

[36] J. T. Sauls, D. Li, and S. Jun, Adder and a coarse-grained approach to cell size homeostasis in bacteria, Curr. Opin. Cell Biol. **38**, 38 (2016).

[37] B. Munsky and M. Khammash, The finite state projection algorithm for the solution of the chemical master equation, J. Chem. Phys. **124**, 044104 (2006).

[38] D. T. Gillespie, A general method for numerically simulating the stochastic time evolution of coupled chemical reactions, J. Comput. Phys. **22**, 403 (1976).

[39] J. Männik, F. Wu, F. J. Hol, P. Bisicchia, D. J. Sherratt, J. E. Keymer, and C. Dekker, Robustness and accuracy of cell division in escherichia coli in diverse cell shapes, Proc. Natl. Acad. Sci. U.S.A. **109**, 6957 (2012).

[40] M. Hashimoto, T. Nozoe, H. Nakaoka, R. Okura, S. Akiyoshi, K. Kaneko, E. Kussell, and Y. Wakamoto, Noise-driven growth rate gain in clonal cellular populations, Proc. Natl. Acad. Sci. U.S.A. **113**, 3251 (2016).

[41] S. Vadia and P. A. Levin, Growth rate and cell size: A re-examination of the growth law, Curr. Opin. Microbiol. **24**, 96 (2015).

[42] S. Iyer-Biswas, C. S. Wright, J. T. Henry, K. Lo, S. Burov, Y. Lin, G. E. Crooks, S. Crosson, A. R. Dinner, and N. F. Scherer, Scaling laws governing stochastic growth and division of single bacterial cells, Proc. Natl. Acad. Sci. U.S.A. **111**, 15912 (2014).

[43] D. Huh and J. Paulsson, Random partitioning of molecules at cell division, Proc. Natl. Acad. Sci. U.S.A. **108**, 15004 (2011).

[44] C. Roubinet, I. J. White, and B. Baum, Asymmetric nuclear division in neural stem cells generates sibling nuclei that differ in size, envelope composition, and chromatin organization, Current Biology **31**, 3973 (2021).

[45] S. M. Hingley-Wilson, N. Ma, Y. Hu, R. Casey, A. Bramming, R. J. Curry, H. L. Tang, H. Wu, R. E. Butler, W. R. Jacobs *et al.*, Loss of phenotypic inheritance associated with ydci mutation leads to increased frequency of small, slow persisters in escherichia coli, Proc. Natl. Acad. Sci. USA **117**, 4152 (2020).

[46] C. A. Vargas-García and A. Singh, Elucidating cell size control mechanisms with stochastic hybrid systems, in *Proceedings of the IEEE Conference on Decision and Control (CDC'18)* (IEEE, Los Alamitos, CA, 2018), pp. 4366–4371.

[47] M. Doumic, A. Olivier, and L. Robert, Estimating the division rate from indirect measurements of single cells, arXiv:1907.05108 (2019).

[48] M. Xia, C. D. Greenman, and T. Chou, Pde models of adder mechanisms in cellular proliferation, SIAM J. Appl. Math. **80**, 1307 (2020).

[49] P. Bokes and A. Singh, Cell volume distributions in exponentially growing populations, in *Proceedings of the International Conference on Computational Methods in Systems Biology* (Springer, Berlin, 2019), pp. 140–154.

[50] E. Bernard, M. Doumic, and P. Gabriel, Cyclic asymptotic behaviour of a population reproducing by fission into two equal parts, Kinetic and Related Models **12**, 551 (2017).

[51] O. Diekmann, H. J. Heijmans, and H. R. Thieme, On the stability of the cell size distribution, J. Math. Biol. **19**, 227 (1984).

[52] See Supplemental Material http://link.aps.org/supplemental/10.1103/PhysRevE.104.044415 for videos showing time dynamics of size distributions

[53] C. Nieto, J. Arias-Castro, C. Vargas-Garcia, C. Sanchez, and J. M. Pedraza, Noise signature in added size suggests bacteria target a commitment size to enable division, bioRxiv 2020.07.15.202879 (2020), doi: 10.1101/2020.07.15.202879.

[54] C. A. N. Acuna, C. A. V. Garcia, and J. M. Pedraza, Stochasticity in bacterial division control: Preliminary consequences for protein concentration, bioRxiv 826867 (2019), doi: 10.1101/826867.

[55] M. Soltani, C. A. Vargas-Garcia, D. Antunes, and A. Singh, Intercellular variability in protein levels from stochastic expression and noisy cell cycle processes, PLoS Comput. Biol. **12**, e1004972 (2016).

[56] P. Thomas, G. Terradot, V. Danos, and A. Y. Weiße, Sources, propagation and consequences of stochasticity in cellular growth, Nat. Commun. **9**, 4528 (2018).

[57] S. Tiruvadi-Krishnan, J. Männik, P. Kar, J. Lin, A. Amir, and J. Mannik, Replication-related control over cell division in escherichia coli is growth-rate dependent (2021), doi: 10.2139/ssrn.3787897.